Chiral symmetry breaking and monopole dynamics in noncompact QED$_3$ coupled to a four-Fermi interaction

Wesley Armour,[1] John B. Kogut,[2] and Costas Strouthos[3]

[1]*Diamond Light Source, Harwell Campus, Didcot, Oxfordshire OX11 0DE, United Kingdom*
[2]*Department of Energy, Division of High Energy Physics, Washington, D.C. 20585, USA, and Department of Physics—TQHN, University of Maryland, 82 Regents Drive, College Park, Maryland 20742, USA*
[3]*Computation-based Science and Technology Research Center, The Cyprus Institute, 1645 Nicosia, Cyprus*

(Received 29 April 2010; published 9 July 2010)

We present results from the first lattice simulations of three-dimensional noncompact quantum electrodynamics (QED$_3$) with N_f four-component fermion flavors coupled to a weak Z_2 chirally invariant four-fermi interaction. Results with $N_f \geq 4$ show that the scaling near the strong coupling chiral transition or sharp crossover is determined by the 3*d* Gross-Neveu ultraviolet-stable renormalization group fixed point. Small deviations of the $N_f = 4$ critical exponents from the respective Gross-Neveu ones, hint at evidence for nonzero fermion mass generated by the gauge fields dynamics that might have been enhanced by the four-fermi coupling. It is also shown that the scaling region is suppressed at weak four-fermi couplings and large N_f values. Measurements of (i) a monopole susceptibility which is the polarizability of the monopole configurations, and (ii) the density of isolated monopoles, imply that for $N_f \geq 1$ and weak gauge couplings the monopoles do not affect the theory's confining properties, because they are shielded.

DOI: 10.1103/PhysRevD.82.014503 PACS numbers: 11.15.Ha, 11.30.Rd, 12.20.Ds

I. INTRODUCTION

Spontaneous chiral symmetry breaking plays a significant role in both particle and condensed matter physics. Of particular interest is the study of quantum field theories in which the ground state shows a sensitivity to the number of fermion flavors N_f. Three-dimensional parity-invariant quantum electrodynamics with four-component spinors is such an interesting and challenging field theory with rich dynamics that resemble four-dimensional QCD and walking technicolor theories [1]. The gauge coupling e^2 has mass dimension one and thus provides the theory with a natural scale that plays a role similar to Λ_{QCD} in four dimensions. This implies asymptotic freedom, since for processes with momentum transfer $k \gg e^2$ the theory is effectively noninteracting.

Nontrivial behavior may arise in the infrared limit, as suggested by an expansion in $1/N_f$ [2]. The theory is believed to exhibit logarithmic confinement of electric charges and chiral symmetry breaking when the number of fermion flavors N_f is smaller than a critical value N_{fc}. Super-renormalizability ensures that QED$_3$ is free from ultraviolet divergences, thus making analytical calculations more transparent. Most analytical approaches, mainly based on self-consistent solutions of Schwinger-Dyson equations (SDE), converge to values of N_{fc} between three and five [3,4]. There are also SDE results which claim that chiral symmetry is broken for all values of N_f [5]. Also, a perturbative analysis of renormalization group flow in the large-N_f limit predicts $N_{fc} \approx 6$ [6]. Recent progress on gauge invariant solutions of SDE has been recently reported in [7]. An argument based on the inequality $f_{IR} \leq f_{UV}$ (where f is the absolute value of the thermodynamic free energy) that can be estimated by counting relevant degrees of freedom in the infrared and ultraviolet limits yields the prediction $N_{fc} \leq \frac{3}{2}$ [8]; a result that was later challenged in [9]. Analytical calculations also predict that at N_{fc} the theory undergoes a conformal phase transition [10], which is a generalization of the infinite-order Berezinskii-Kosterlitz-Thouless transition in two dimensions.

Lattice simulations provided evidence that chiral symmetry is broken for $N_f < 1.5$ [11–13], whereas $N_f = 2$ appeared chirally symmetric [13,14] on lattices with physical extent up to $Le^2 \approx 90$. The principal obstruction to a definitive answer has been the separation of scales in the theory, i.e. the fermion dynamical mass is at least an order of magnitude smaller than the natural scale e^2 [15] which is of the order of the momentum cutoff given by the inverse lattice spacing. In addition, large finite volume effects resulting from the presence of a massless photon in the spectrum prevent a reliable extrapolation to the thermodynamic limit. Analytical results claimed that to detect chiral symmetry breaking for $N_f \geq 1.5$ lattice volumes much bigger than the ones currently used in numerical simulations are required [4,16]. Another possibility is that, based on universality arguments, the infrared limit of QED$_3$ may be equivalent to the 3*d* Thirring model at its strong coupling ultraviolet-stable renormalization group fixed point, as both models are chirally invariant under the same $U(2N_f)$ group. This universality argument can be valid provided in the Thirring model the interaction is mediated by a massless vector boson [17], which still needs to be checked rigorously in lattice simulations. So far, numerical

 © 2010 The American Physical Society

simulations of the Thirring model predicted that $N_{fc} = 6.6(1)$ [18].

The existence of a critical number of flavors N_{fc} in QED_3 can be explained by the following semiclassical arguments discussed in [19] and also reviewed in [12]. In the large-N_f limit the photon propagator is modified by the vacuum polarization diagram from $1/k^2$ to $1/[k^2 + \frac{g^2}{8}N_f k]$ [20]. The super-renormalizable theory is rapidly damped in the ultraviolet regime and all interesting dynamics are expected in the infrared limit, where the dimensionless interaction strength scales as $1/N_f$. Naively, one could deduce that the confining property of the Coulomb potential is screened by virtual fermion-antifermion pairs, because in the coordinate space the interaction is modified to $1/r$ for distances $r \gg (e^2 N_f)^{-1}$. However, as discussed in [19] the kinetic energy of fermion-antifermion pairs is positive and scales as r^{-1} by the uncertainty principle. In the infrared, therefore, both kinetic and potential terms scale as r^{-1} and it becomes a delicate question which dominates. Since when $r \to 0$ the positive kinetic term must dominate the logarithmic Coulomb term, we deduce in this case the existence of an energy minimum at some nonzero r, implying the existence of stable fermion-antifermion bound states in the ground state. This semiclassical argument suggests a nonvanishing chiral condensate for $N_f < N_{fc}$. For asymptotically large r the massive fermions decouple, ceasing to screen the charge, and the logarithmically confining Coulomb potential is restored. For $N_f > N_{fc}$ the theory is conformal, consisting of massless fermions interacting via a $1/r$ potential.

Since the early 1990s, noncompact QED_3 with or without extra four-fermi terms has attracted attention [21,22] because of potential applications to models of high T_c superconductivity. More recently, interest in this model has been revived by suggestions that QED_3 with two fermion flavors may be an effective theory for the underdoped and nonsuperconducting region of the phase diagram of high-T_c superconducting cuprate compounds [23]. In this sense, the abstract theoretical problem of the value of N_{fc} assumes phenomenological importance. These results have also stimulated lattice simulations of QED_3 with Fermi and gap anisotropies [24].

In this paper we present the first exploratory lattice simulation results of parity-invariant noncompact QED_3 with massless fermions. This is achieved with the introduction of a four-fermi interaction in the QED_3 action. The Lagrangian for the continuum Euclidean field theory is given by

$$\mathcal{L} = \bar{\psi}_i(\not{\partial} - ie\gamma_\mu A_\mu + m)\psi_i - \frac{g_s^2}{2N_f}(\bar{\psi}_i\psi_i)^2 + \frac{1}{4}F_{\mu\nu}F_{\mu\nu}, \tag{1}$$

with the index i implying a summation over N_f four-component fermion flavors. The introduction of the four-fermi interaction reduces the $U(2N_f)$ chiral symmetry of QED_3 to a discrete Z_2 symmetry: $\psi_i \to \gamma_5\psi$; $\bar{\psi}_i \to -\bar{\psi}\gamma_5$. For computational purposes it is useful to introduce the auxiliary field $\sigma \equiv g_s^2\bar{\psi}_i\psi_i$, and the semibosonized Lagrangian becomes

$$\mathcal{L} = \bar{\psi}_i(\not{\partial} - ie\gamma_\mu A_\mu + \sigma + m)\psi_i + \frac{N_f}{2g_s^2}\sigma^2 + \frac{1}{4}F_{\mu\nu}F_{\mu\nu}. \tag{2}$$

Both the noncompact [25] and compact [26] lattice versions of this model have been used successfully to show that QED_4 is a logarithmically trivial theory and the systematics of the logarithms of triviality follow those of the NJL model rather than those of the scalar $\lambda\phi^4$ theory. In the formulation of Eq. (2) the σ field acts as a chiral order parameter which receives a vacuum expectation value, proportional to the chiral condensate, in the chirally broken phase. The Dirac operator is now nonsingular even with $m = 0$ and its inversion is very fast.

The three- and four-dimensional versions of the theory are very different from each other, as in $3d$ the four-fermi interaction is a relevant operator. It is well known that the $3d$ Gross-Neveu model (GNM_3), although nonrenormalizable in weak coupling perturbation theory, becomes renormalizable in the $1/N_f$ expansion [27]. At sufficiently strong couplings and large-N_f chiral symmetry is spontaneously broken in GNM_3, leading to a dynamically generated fermion mass $\Sigma = \langle\sigma\rangle \gg m$. The critical coupling g_{sc}^2 at which the gap $\Sigma/\Lambda_{UV} \to 0$ defines an ultraviolet-stable renormalization group fixed point at which an interacting continuum limit may be taken. As the gauge coupling is varied and the four-fermi coupling is fixed at some value $g_s^2 < g_{sc}^2$, then depending on the value of N_f the model is expected to undergo either a chiral phase transition or a sharp crossover from a strong coupling phase (where $\langle\bar{\psi}\psi\rangle \neq 0$) to a weak coupling phase where $\langle\bar{\psi}\psi\rangle$ is either zero or very small and possibly undetectable in current lattice simulations. Hereafter, we will use the term "chiral transition" to denote either a chiral phase transition or a sharp crossover from strong to weak gauge couplings. Unlike what happens in $4d$, here near the transition, the weak four-fermi term is expected to play a dominant role as compared to the ultraviolet-finite gauge interaction. Understanding the role of the weak four-fermi coupling in lattice simulations of noncompact QED_3 is one of the main themes of this paper. Preliminary results were presented in [28]. Emphasis is also placed on the dynamics of monopoles (which in $3d$ are instantons) at both strong and weak couplings and try to understand whether they affect the confining properties of the model. The interplay of fermions and magnetic monopoles was recently studied in numerical simulations of the compact lattice version of this model [29]. The authors of [29] provided evidence that

for $N_f = 4$ the monopole plasma persists even at weak gauge couplings. In noncompact QED_3, however, the role of topological excitations may be different, because in this case the Dirac strings carry a nonvanishing contribution to the pure gauge part of the action [30].

The paper is organized as follows. In Sec. II, we introduce the staggered fermion lattice action and the monopole observables. In Sec. III we present results related to the strong coupling chiral transition such as estimates of the critical exponents β_m and δ for $N_f = 4$ and show that they are close to the respective GNM_3 values, implying that the transition is dominated by the ultraviolet-stable GNM_3 fixed point. Small but systematic deviations of the values of β_m and δ from the GNM_3 exponents hint at preliminary evidence of nonzero fermion mass generated by the gauge field dynamics at weak gauge couplings. We also show that the scaling region is suppressed at weak four-fermi couplings and large N_f. Subsequently, we show that at strong gauge couplings the monopole density has a weak dependence on the values of the four-fermi coupling. We then study the behavior of the monopole susceptibility χ_m (defined by Cardy in [31]) for $N_f = 1, \ldots, 12$ and within the accuracy of our data we observe no diverging behavior in χ_m with the lattice volume, implying that monopoles and antimonopoles are shielded in the continuum limit. Further evidence in favor of this scenario is provided by the density of isolated monopoles (positive magnetic charges that do not have any antimonopoles in the nearest neighborhood) which decays faster with the inverse gauge coupling than the total density of positive magnetic charges. In Sec. IV, we summarize and discuss our main findings and also point to possible future extensions of this work.

II. LATTICE MODEL AND OBSERVABLES

In this first exploratory study of noncompact QED_3 with a four-fermi term, we have chosen the simplest Z_2 chirally invariant four-fermi interaction which for practical purposes is preferable over terms with a continuous chiral symmetry, because the latter are not as efficiently simulated due to massless modes in the strongly cut-off theory. The lattice action using staggered lattice fermion fields χ, $\bar{\chi}$ is given by the following equations:

$$S = \frac{\beta}{2} \sum_{x,\mu<\nu} F_{\mu\nu}(x) F^{\mu\nu}(x) + \sum_{x,x'} \bar{\chi}(x) Q(x,x') \chi(x') + \frac{N_f \beta_s}{4} \sum_{\tilde{x}} \sigma^2(\tilde{x}), \tag{3}$$

where

$$F_{\mu\nu}(x) \equiv \alpha_\mu(x) + \alpha_\nu(x+\hat{\mu}) - \alpha_\mu(x+\hat{\nu}) - \alpha_\nu(x), \tag{4}$$

$$Q(x,x') \equiv \frac{1}{2} \sum_\mu \eta_\mu(x) [\delta_{x',x+\hat{\mu}} U_{x\mu} - \delta_{x',x-\hat{\mu}} U^\dagger_{x-\hat{\mu},\mu}] + \delta_{xx'} \frac{1}{8} \sum_{\langle \tilde{x}, x \rangle} \sigma(\tilde{x}) + m \delta_{xx'}. \tag{5}$$

The indices x, x' consist of three integers (x_1, x_2, x_3) labelling the lattice sites, where the third direction is considered to be timelike. The symbol $\langle \tilde{x}, x \rangle$ denotes the set of the eight dual lattice sites $\tilde{x}$ surrounding the direct lattice site x. Since the pure gauge action is unbounded from above, Eq. (3) defines the *noncompact* formulation of lattice QED. The $\eta_\mu(x)$ are the Kawamoto-Smit staggered fermion phases $(-1)^{x_1 + \cdots + x_{\mu-1}}$, designed to ensure relativistic covariance of the Dirac equation in the continuum limit. The boundary conditions for the fermion fields are antiperiodic in the timelike direction and periodic in the spatial directions. The phase factors in the fermion bilinear are defined by $U_{x\mu} \equiv \exp(i\alpha_{x\mu})$, where $\alpha_{x\mu}$ is the gauge potential. In terms of continuum quantities, $\alpha_{x\mu} = aeA_\mu(x)$, $\beta \equiv \frac{1}{e^2 a}$, $\beta_s \equiv \frac{a}{g_s^2}$ where a is the physical lattice spacing. Because of the noncompact nature of the gauge fields, the nonfermionic part of the action is invariant under gauge transformations defined by the group of real numbers R. The fermionic part remains invariant under the smaller gauge group $R/Z \sim U(1)$. The four-fermi term explicitly breaks the $U(N_f/2) \times U(N_f/2)$ chiral symmetry of the lattice QED_3 action to a discrete Z_2 chiral symmetry.

Performing simulations with massless fermions even with the reduced Z_2 chiral symmetry has substantial advantages, both theoretical and practical. The theory has the exact symmetry of the interaction terms, which forbid chiral symmetry breaking counterterms from appearing in its effective action. In addition, because of the large nonzero vacuum expectation value of the σ field at strong gauge couplings[1] or its fluctuations at weak couplings, the model can be simulated very efficiently. Another advantage of simulations directly in the chiral limit is that we do not have to rely on often uncontrolled chiral extrapolations to measure the chiral condensate.

The simulations were performed with the standard Hybrid Molecular Dynamics (HMD) R algorithm. We used conservatively small values for the HMD trajectory time-step dt and ensured that any $\mathcal{O}(dt^2)$ systematic errors are smaller than the statistical errors on different observables. Among the various parameters used the ones that are the most susceptible to algorithmic systematic errors are those near the $N_f = 4$ chiral transition ($\beta = 0.145$) on the largest lattice volume 42^3, with the weakest four-fermi coupling $\beta_s = 16$. By comparing the values of different observables obtained from simulations with these parameters and with $dt = 0.00125$ and $dt = 0.0025$ we found

[1] At large couplings, pure QED_3 simulations are dramatically slowed down by the strong gauge field flusctuations.

agreement within statistical errors. Therefore, we decided to use $dt = 0.0025$ for all 42^3 and 32^3 simulations. For the smaller lattices 16^3, 24^3 and $N_f \geq 4$ we found that $dt = 0.01$ and 0.005 are small enough to suppress algorithmic systematic errors at strong coupling and weak gauge couplings, respectively. For $N_f \leq 2$ we used $dt = 0.005$ and $dt = 0.0025$ for simulations on 16^3 and 24^3 lattices, respectively.

The magnetic monopoles in the lattice model are identified following the standard DeGrand and Toussaint approach [32]. The plaquette angles $\Theta_{\mu\nu}$ are written as

$$\Theta_{\mu\nu} = \bar{\Theta}_{\mu\nu} + 2\pi s_{\mu\nu}(x), \tag{6}$$

where $\bar{\Theta}_{\mu\nu}$ lie in the range $(-\pi, \pi]$ and $s_{\mu\nu}(x)$ is an integer that determines the flux due to a Dirac string passing through a plaquette. The integer number of monopole charges on the dual lattice sites $\tilde{x}$ is then given by

$$M(\tilde{x}) = \epsilon_{\mu\nu\lambda}\Delta_\mu s_{\nu\lambda}(\tilde{x}), \tag{7}$$

where Δ_ν is the lattice derivative and $M \in \{0, \pm 1, \pm 2\}$. Since on a three-torus the number of monopoles is equal to the number of antimonopoles we define the density of monopole charges as

$$\rho_M = \frac{1}{V}\sum_{\tilde{x}} |M(\tilde{x})|. \tag{8}$$

We also measured the monopole susceptibility χ_m introduced by Cardy [31]:

$$\chi_m = -\frac{1}{V}\sum_r \langle r^2 M(0)M(r)\rangle. \tag{9}$$

This observable is the polarizability of the monopole configurations and if the magnetic charges are in a plasma phase, then χ_m diverges implying that external magnetic fields are shielded. A finite χ_m implies that monopoles and antimonopoles form tightly bound molecules. The observable χ_m has been rarely used in simulations with dynamical fermions, because it is very noisy due to near cancellations of monopole-monopole and monopole-antimonopole contributions. With the inclusion of the four-fermi term in the QED_3 action the algorithm became very efficient and χ_m has been measured with an acceptable signal-to-noise ratio even at relatively strong gauge couplings.

III. RESULTS

In the infinite gauge coupling limit $\beta \to 0$, it is known rigorously that chiral symmetry is broken [33] for values of N_f below a certain critical value. Simulations of QED_3 with staggered fermions and $\beta = 0$ have shown that the theory undergoes a second-order phase transition at $N_f \approx 8$ with mean field theory exponents [19]. Therefore, as β increases, for $N_f > N_{fc}$ there must exist a chiral symmetry restoring phase transition at some finite β_c. For $N_f < N_{fc}$, since the order parameter is very small in the continuum limit, the relic of the transition may persist as a very sharp crossover between weak and strong couplings with a tail of an exponentially suppressed $\bar{\psi}\psi$ extending to weak gauge couplings.[2] For example, for $N_f = 4$, which is the flavor number used in the bulk of our simulations the SDE approaches predict that the value of the dimensionless chiral condensate $\beta^2\langle\bar{\psi}\psi\rangle$ is somewhere between zero and $\mathcal{O}(10^{-4})$ [3]. In this study we assume that a transition takes place at some strong (pseudo-)critical gauge coupling β_c which depends on β_s and we use standard scaling relationships for a second-order phase transition to extract critical exponents. We chose $N_f = 4$, instead of a larger N_f value, because as we show later in this section for large N_f values the width of the scaling region is suppressed.

One of the main goals of this first set of lattice simulations of noncompact QED_3 with the additional four-fermi term is to understand the impact of the Gross-Neveu coupling on the chiral transition. As already mentioned in Sec. I, in $3d$ the four-fermi term becomes a relevant interaction (as opposed to the $4d$ theory where it is an irrelevant interaction) and therefore this term may play a significant role near the chiral transition even at very small values of g_s^2. Given that the pure $3d$ Gross-Neveu model with $N_f = 4$ undergoes a second-order phase transition at $\beta_{sc} = 0.835(1)$ [34], we chose $\beta_s = 2$, 4, 8, 16 for the $N_f = 4$ strong gauge coupling simulations. All these values of β_s are in the symmetric phase of the Gross-Neveu model, implying that they cannot generate nonzero fermion dynamical mass on their own. The finite volume effects are expected to increase with β_s and in the limit $\beta_s \to \infty$, on finite size lattices $\langle\bar{\chi}\chi\rangle \to 0$. In order to check the extent of finite volume effects, we performed simulations on 16^3 and 24^3 lattices for $\beta_s = 2$, on 32^3 lattices for $\beta_s = 4$, 8 and on 32^3 and 42^3 lattices for $\beta_s = 16$. It is clear from the data for $\langle\bar{\chi}\chi\rangle$ versus β shown in Fig. 1 that the 24^3 lattice size is sufficiently large to suppress finite volume effects for $\beta_s = 2$. Also a comparison of the values of $\langle\bar{\chi}\chi\rangle$ from simulations with $\beta_s = 16$ on 32^3 and 42^3 lattices implies that 32^3 is large enough to suppress finite size effects for $\beta_s = 4$, 8, 16. We fitted the data for the different β_s values to the standard scaling relation of a second-order transition order parameter:

$$\langle\bar{\chi}\chi\rangle = a(\beta_c - \beta)^{\beta_m}. \tag{10}$$

The fitting range was varied to ensure that all the data near the transition that give stable values for β_m and β_c were included. For the weakest four-fermi coupling $\beta_s = 16$ the three parameter fits to Eq. (10) did not give stable values for β_m and β_c when the fitting range was varied. This is attributed to the fact that for such a very weak four-fermi coupling the scaling window is very narrow. Therefore, in

[2]This may not be directly detectable in lattice simulations.

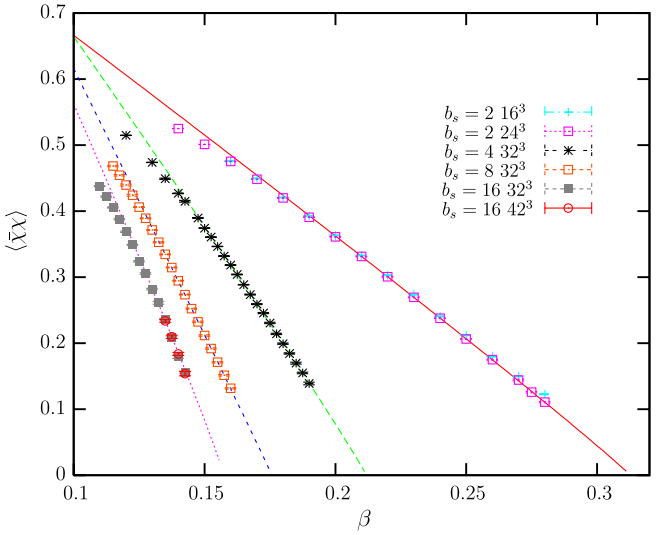

FIG. 1 (color online). Fits of $\langle\bar{\chi}\chi\rangle$ vs β to Eq. (10) for $N_f = 4$ and $\beta_s = 2, 4, 8, 16$.

order to obtain an estimate for β_c and the width of the scaling region we fixed $\beta_m = 0.93$ (the value of the $3d$ Gross-Neveu exponent [34]) and performed two-parameter fits with Eq. (10). A reasonable fit ($\chi^2/\text{dof} = 1.3$) was obtained from the data in the range $\beta = [0.1275 - 0.140]$. All the results from this analysis, namely, the values for β_c, β_m, and the fitting ranges (where β_{cross} is a crossover coupling that signals the beginning of the scaling region) are shown in Table I. It is deduced that the values of β_m are in good agreement (or slightly larger by 1–2 standard deviations) with the $\beta_m = 0.93(3)$ of the $N_f = 4$ GNM$_3$ [34]. An analytical calculation based on SDE and large-N_f approaches for QED$_3$ with a $U(1)$ chirally invariant four-fermi term [35] predicted that for $N_f > N_{fc} = 112/3\pi^2$ the magnetic critical exponent is $\beta_m = (3 - 2a)/4a$, where $a = \frac{1}{2}\sqrt{1 - N_{fc}/N_f}$. This result reproduces the GNM$_3$ exponent $\beta_m = 1$ only when $N_f \gg N_{fc}$.

Our results for the critical coupling show that β_c decreases as the four-fermi coupling gets weaker and it is expected to saturate to an asymptotic value in the limit $\beta_s \to \infty$. This asymptotic value is clearly smaller than $\beta_c = 0.212(4)$ obtained from pure QED$_3$ simulations with $N_f = 4$ [12]. The discrepancy in the estimates of β_c between the two models is attributed to the presence of lattice discretization counter-terms in the pure QED$_3$ effective action, which are forbidden by the introduction of the four-fermi term in the current model. It should be noted that for the same reason the inclusion of the four-fermi term in the noncompact QED$_4$ Lagrangian led to a larger scaling window in the direction of the gauge coupling than in pure noncompact QED$_4$ [25]. Another interesting result shown in the last column of Table I is that the Gross-Neveu scaling region ($\beta_c - \beta_{\text{cross}}$) is suppressed as the four-fermi coupling becomes weaker. This can be understood by a combination of dimensional analysis and scaling arguments as follows. The fixed four-fermi coupling g_s^2 with mass dimension -1 introduces a new scale in the system. As the scaling region is approached by increasing β, the magnitude of the dimensionless gauge coupling at the crossover into the scaling region $e^2_{\text{cross}}a$ (a is the lattice spacing) becomes comparable to the magnitude of the dimensionless four-fermi coupling $g_s^2 a^{-1}$. Therefore, $e^2_{\text{cross}} m_e^2 \sim g_s^2$, where m_e is the electron mass which is an inverse correlation length and obeys the scaling relation:

$$m_e^{\text{cross}} = d(\beta_s)(\beta_c - \beta_{\text{cross}})^{\nu}, \tag{11}$$

with $\nu = 1.0$ for the $N_f = 4$ GNM$_3$ [34]. In the large β_s limit, $d(\beta_s)$ and β_{cross} saturate to certain values, implying

$$(\beta_c - \beta_{\text{cross}}) \sim \sqrt{\frac{1}{\beta_s}}. \tag{12}$$

It can be seen from the last column of Table I that the data for the scaling region width comply relatively well with Eq. (12), especially for the two weakest four-fermi couplings $\beta_s = 8, 16$.

We also performed simulations on 32^3 lattices with nonzero fermion bare mass in the range $m = 0.005, \ldots, 0.020$ at the respective critical gauge couplings for $\beta_s = 2, 4, 8, 16$. The results for the chiral condensate as a function of m were fitted to the standard scaling relation:

$$\langle\bar{\chi}\chi\rangle = cm^{1/\delta}. \tag{13}$$

The data and the fitting functions are shown in Fig. 2 and the values of the critical exponent δ are presented in Table II. The extracted values of δ are close (within 1–2 standard deviation) to the $N_f = 4$ GNM$_3$ $\delta = 2.24(11)$ [34]. The slightly larger values of δ in Table II as compared to the pure GNM$_3$ value could be attributed to either the accuracy with which the critical couplings were measured and/or to a small fermion mass generated by the gauge field dynamics. Notably the $\delta = 2.45(3)$ extracted from simulations with the strongest four-fermi coupling $\beta_s = 2$ hints at preliminary evidence in favor of mass generation by the QED$_3$ dynamics that might have been enhanced by the four-fermi coupling. Future better precision simulations may further clarify this issue. Nevertheless, the two critical exponents β_m and δ are sufficient to define the universal properties of the model at (pseudo-)criticality, since all the other exponents can be estimated using standard hyperscaling relations. These results clearly indicate that the

TABLE I. Results from fits of $\langle\bar{\chi}\chi\rangle$ vs β to Eq. (10).

β_s	Fitting range	β_c	β_m	$(\beta_c - \beta_{\text{cross}})$
2	0.22–0.28	0.313(2)	0.96(3)	0.09(1)
4	0.16–0.19	0.212(2)	0.96(4)	0.052(5)
8	0.1325–0.16	0.176(1)	0.99(3)	0.044(3)
16	0.1275–0.14	0.1579(4)	0.93 (fixed)	0.031(3)

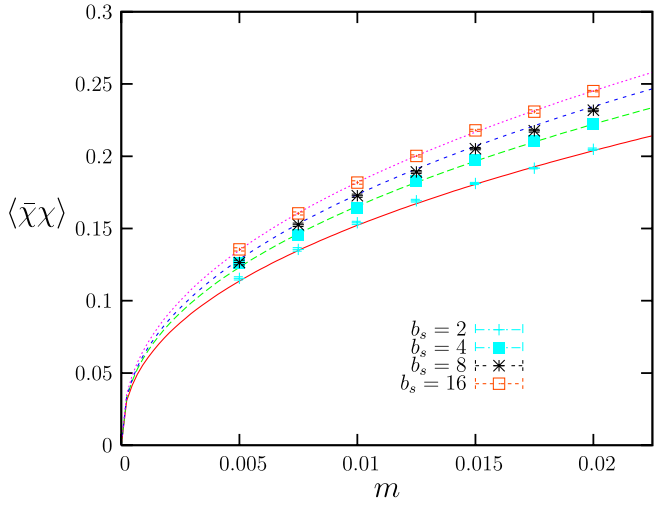

FIG. 2 (color online). Fits of $\langle\bar{\chi}\chi\rangle$ vs m to Eq. (13) for $N_f = 4$ and $\beta_s = 2, 4, 8, 16$.

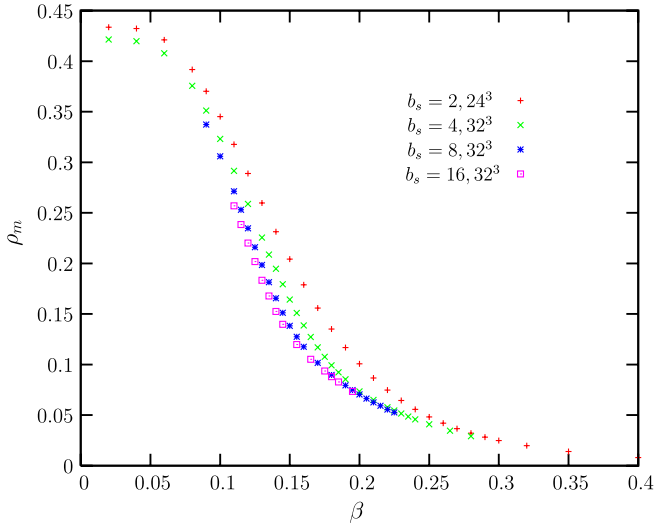

FIG. 3 (color online). ρ_m vs β for $N_f = 4$ and $\beta_s = 2, 4, 8, 16$.

four-fermi interaction plays a predominant role in the scaling of the order parameter near the chiral transition. Although the transition may be approached by varying the gauge coupling alone, as mentioned in Sec. I pure QED_3 is super-renormalizable and ultraviolet-finite, and therefore the ultraviolet-stable fixed point of GNM_3 determines the scaling properties of the transition. This situation is similar to the Higgs-Yukawa model where the interaction $\lambda\phi^4$ is also super-renormalizable in $3d$, and the four-fermi interaction determines the model's universality class [36]. An analogous result was recently obtained in a perturbative renormalization group theory approach of the graphene phase diagram [37], where it was shown that in the presence of a four-fermi interaction the electron charge is rendered more marginally irrelevant than at the Gaussian fixed point.

In Fig. 3 we present the results for the monopole density ρ_m versus β for $\beta_s = 2, 4, 8, 16$. We see that ρ_m decreases monotonically and smoothly with β with no evidence for any abrupt changes at the chiral transition couplings that might signal the existence of a phase transition from strong to weak couplings. At strong gauge couplings ρ_m decreases as β_s increases and above the chiral transition ρ_m tends to become β_s-independent. It should be noted, however, that the impact of β_s on ρ_m is significantly smaller than on the chiral condensate (see Fig. 1); a similar result was obtained in simulations of the compact version of the model [29]. As expected, a stronger four-fermi coupling produces a larger enhancement of the fermion condensate near the transition, whereas the monopole dynamics are mainly determined by the short-distance fluctuations of the gauge fields.

In order to study the dependence of the scaling region width on N_f we performed additional simulations with $N_f = 8$, 12 and $m = 0$, $\beta_s = 2$ on 24^3 lattices. It is shown in Fig. 4 that as N_f increases the values of $\langle\bar{\chi}\chi\rangle$ decrease, due to the enhanced screening of the electromagnetic interaction by virtual fermion-antifermion pairs. The data for $\langle\bar{\chi}\chi\rangle$ were fitted to Eq. (10) in the regions where stable values for β_m and β_c were obtained. The results for $N_f = 8$, 12 together with the $N_f = 4$ results discussed earlier,

TABLE II. Results for exponent δ extracted from fits to Eq. (13) for $N_f = 4$.

β_s	δ
2	2.45(3)
4	2.36(3)
8	2.34(3)
16	2.33(2)

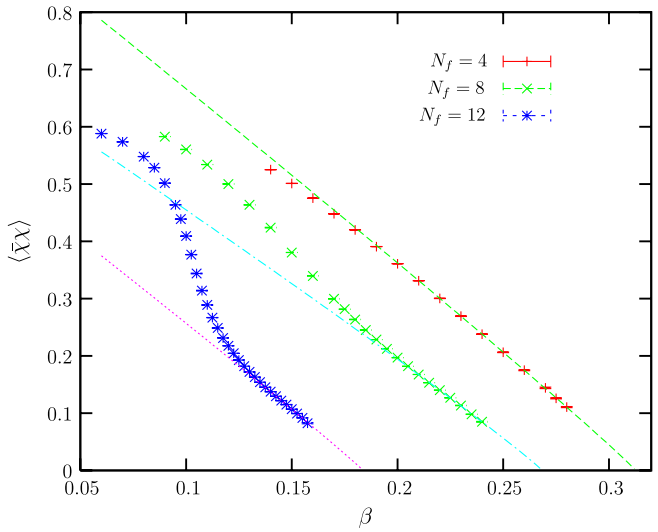

FIG. 4 (color online). $\langle\bar{\chi}\chi\rangle$ vs β for $N_f = 4$, 8, 12.

TABLE III. Results from fits of $\langle\bar{\chi}\chi\rangle$ vs β to Eq. (10) for $N_f = 4, 8, 12$ and compliance of the width of the scaling region to Eq. (14).

N_f	Fitting range	β_c	β_m	$R \equiv (\beta_c - \beta_{\text{cross}})$	$R/\sqrt{\frac{\beta_{\text{cross}}(N_f)}{N_f}}$
4	0.22–0.28	0.313(2)	0.96(3)	0.093(8)	0.40(9)
8	0.21–0.24	0.269(3)	0.95(6)	0.059(5)	0.36(7)
12	0.140–0.1575	0.184(3)	0.97(11)	0.044(5)	0.41(6)

and the fitted curves are shown in Fig. 4 and summarized in Table III. The values of β_c decrease as N_f increases and the values of the magnetic critical exponent β_m are close to the large-N_f GNM_3 value $\beta_m = 1$. As already mentioned in Sec. I the dimensionless strength of the QED_3 interaction is given by $\sim 1/N_f$. Following the reasoning that led to the derivation of Eq. (12), it can be easily shown that for fixed β_s and variable N_f the width of the Gross-Neveu scaling region is given by

$$(\beta_c - \beta_{\text{cross}}) \sim \sqrt{\frac{\beta_{\text{cross}}(N_f)}{N_f}}, \tag{14}$$

where $\beta_{\text{cross}}(N_f)$ is the crossover coupling into the GNM_3 scaling region. The results presented in Table III show that the scaling region is suppressed for large N_f values. It is also inferred from the results in the last column of Table III that the data comply with Eq. (14) relatively well. In a similar way to the chiral condensate, the monopole excitations density shown in Fig. 5 also gets smaller as the interaction strength is decreased by increasing N_f. It is also interesting to observe that in Fig. 6 the data for $\langle\bar{\chi}\chi\rangle$ versus ρ_m for $N_f = 4$, 8, 12 and $\beta_s = 2$ collapse on a single curve, the only exception being the $N_f = 4$ data at small values of ρ_m, a regime that coincides with the broader $N_f = 4$ GNM_3 scaling region. We infer from Fig. 6 that large N_f values and strong gauge couplings produce chiral condensation and topological excitations in a very similar almost N_f-independent manner, without this implying anything about the impact of monopoles on the theory's confining properties. From the monopole density alone one cannot reach conclusions regarding the confining properties of the theory.

Next, we take a closer look at the monopole dynamics by discussing results for the monopole susceptibility χ_m defined in Eq. (9). This observable is far more informative than ρ_m, because it measures the polarizability of the monopole configurations and it is expected to show a diverging behavior if the monopoles and antimonopoles are in a plasma phase. As mentioned in Sec. II, χ_m is in general very noisy due to near cancellations of monopole-monopole and monopole-antimonopole contributions. However, the four-fermi term introduced in the QED_3 action substantially increased the efficiency of the simulation algorithm and enabled us to measure χ_m with acceptable signal-to-noise ratio even at relatively strong couplings. The data for χ_m versus β obtained from simulations with $N_f = 4$, $\beta_s = 2$ on 16^3, 24^3 and 32^3 lattices are presented in Fig. 7. Although χ_m increases monotonically with the gauge coupling, there are no signs of a

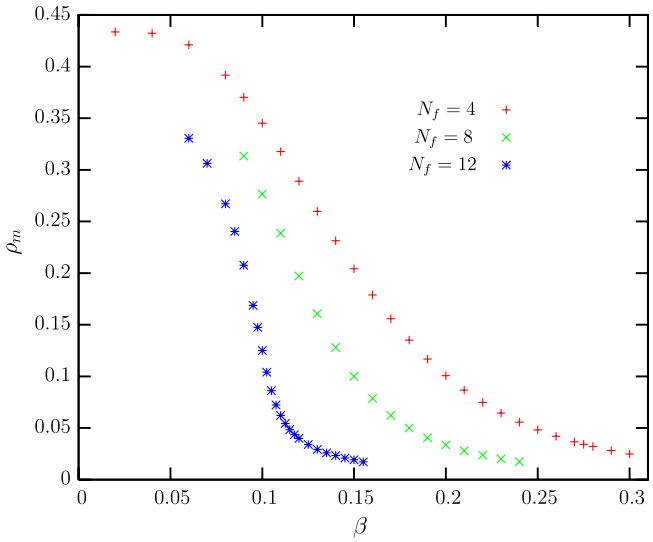

FIG. 5 (color online). Monopole density ρ_m vs β for $N_f = 4$, 8, 12, $\beta_s = 2$.

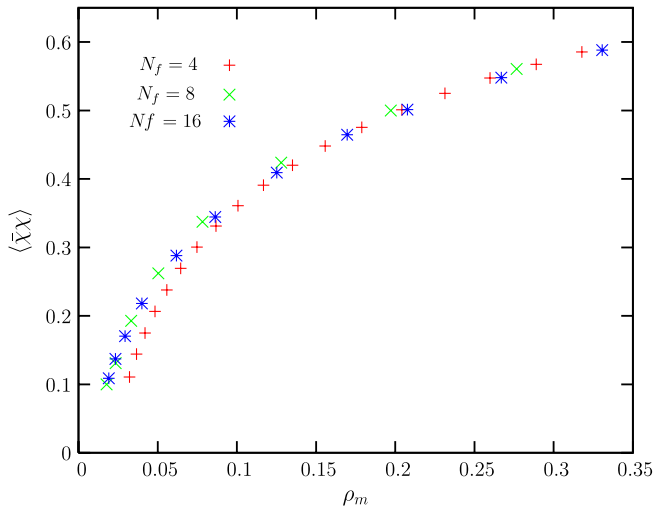

FIG. 6 (color online). (Color online) $\langle\bar{\chi}\chi\rangle$ vs ρ_m for $N_f = 4$, 8, 12 and $\beta_s = 2$.

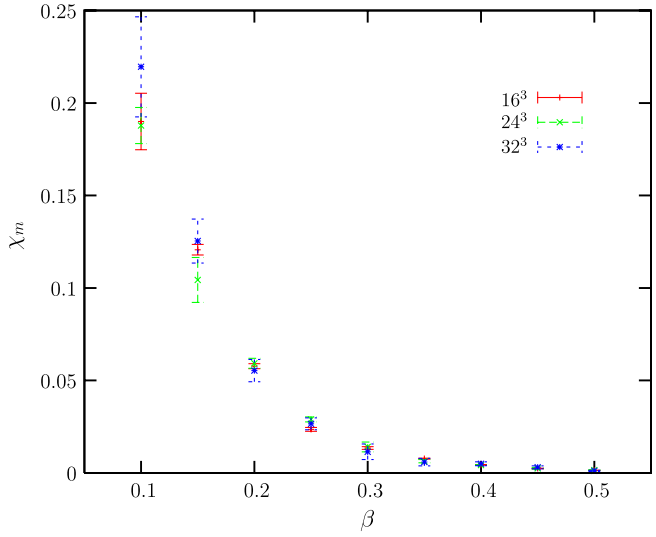

FIG. 7 (color online). χ_m vs β for $N_f = 4$, $\beta_s = 2$ on 16^3, 24^3, and 32^3 lattices.

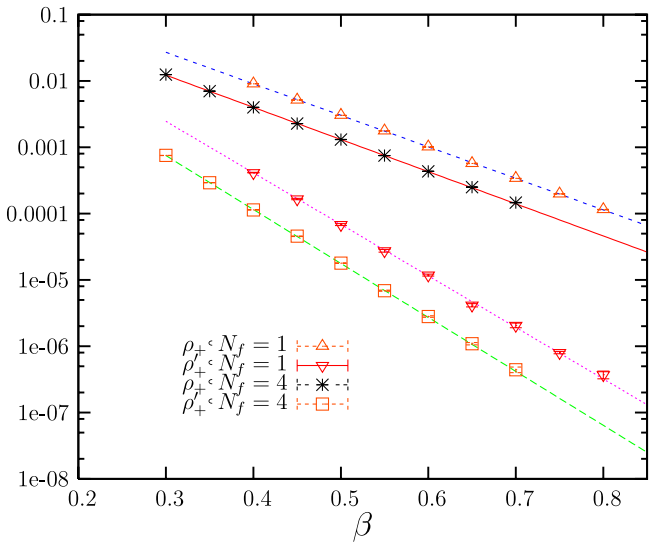

FIG. 9 (color online). Positive monopole charges density ρ_+ and isolated positive monopole charges density ρ'_+ vs β for $N_f = 1, 4$, $\beta_s = 2$ on 32^3 lattice.

divergent behavior. These results imply that monopoles are shielded by forming tightly bound molecules. We also performed simulations with different numbers of fermion flavors in the range $N_f = 1, 2 \ldots, 12$ on 16^3 and 24^3 lattices with $\beta_s = 2$. The values of $\beta = 0.4, 0.5$ used are in the weak coupling phase for all N_f values in the sense that $\langle \bar{\psi}\psi \rangle$ is consistent with zero and the effective order parameter $\langle |\bar{\psi}\psi| \rangle$ decreases with the lattice volume. Again, the data for χ_m presented in Fig. 8 show no signs of a diverging behavior as they are independent of the lattice volume within statistical errors. These results imply that for $N_f \geq 1$ the monopole dynamics do not affect the confining properties of the theory's continuum limit.

The conclusion of the previous paragraph is strengthened by the data in Fig. 9, where we show for $N_f = 1$ and 4

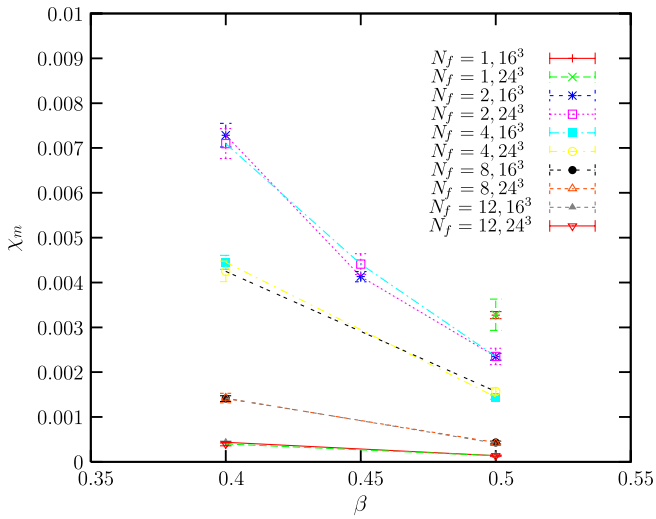

FIG. 8 (color online). χ_m vs β for $N_f = 1, 2, \ldots, 12$, $\beta_s = 2$ on 16^3 and 24^3 lattices.

the density of positive magnetic charges (monopoles) ρ_+ and the density of monopoles without any antimonopoles in their nearest neighborhood $(x_i \pm 1)$ ρ'_+ versus beta. We fitted these data to an empirical function $f(\beta) = a_1 \exp(-a_2\beta)$, and the extracted values of a_2 and a'_2 for ρ_+ and ρ'_+, respectively, are shown in Table IV. The fact that ρ'_+ decays faster than ρ_+ confirms the scenario that at weak couplings the monopoles are shielded. The increase of χ_m and ρ'_+ at strong gauge couplings and/or small N_f values can be easily understood in terms of the renormalization group invariant Dirac quantization condition $eg = e_R g_R$ [38] (g and g_R are the monopole bare and renormalized charges). As N_f (or β) decreases the interaction between fermions and antifermions gets stronger, implying that the monopole-antimonopole attraction gets weaker.

The monopole dynamics in the compact and noncompact formulations may be different at weak couplings and small N_f values, because in the noncompact version the Dirac strings carry a nonvanishing contribution to the pure gauge part of the action [30]. The two formulations, however, become identical in the infinite gauge coupling ($\beta \to 0$) and/or large-N_f ($N_f \to \infty$) limits, as in these limits the fermionic sector with compact gauge links in the action dominates the dynamics. The results from simulations of compact QED$_3$ coupled to a four-fermi term with $N_f = 4$

TABLE IV. Results from fits of ρ_+ and ρ'_+ vs β to $f(\beta) = a_1 \exp(-a_2\beta)$ for $N_f = 1, 4$.

N_f	1	4
a_2	10.9(1)	11.16(4)
a'_2	17.90(9)	18.74(3)

[29] provided evidence that the monopole plasma phase persists even at weak gauge couplings. Although our simulations with $N_f = 4$ were performed at relatively strong couplings deep in the chirally broken phase, it is unclear whether we reached the limit where the monopole dynamics in the two formulations should become similar. Furthermore, it has been suggested [39,40] that the compact and noncompact formulations may be equivalent. This suggestion was largely based on comparisons of chirally extrapolated data for $\langle\bar{\chi}\chi\rangle$ versus ρ_m from the two models. The authors of [40] also suggested that even at weak couplings the monopoles in noncompact QED_3 may exist in a plasma phase. Our results and their difference from those reported in [29] imply that these suggestions may not be valid. Marston [41] and later on Kleinert and collaborators [42,43] suggested in a series of analytical papers on compact QED_3 that above a certain critical number of fermion flavors (N_{fc}) a phase exists where the monopole-antimonopole potential is modified from $1/r$ to $\ln(r)$, implying that monopoles are shielded and do not influence the continuum limit. Recently, it was reported that $N_{fc} = 36$ [43]. Also Herbut and collaborators [44] claimed that in compact QED_3, the interaction among magnetic dipole pairs restores the Coulomb potential at large distances, and the monopoles are in a plasma phase at all $\beta < \infty$ and $N_f < \infty$. In the near future we plan to simulate compact QED_3 with different N_f values and compare the results for monopole dynamics with those mentioned above.

IV. SUMMARY AND OUTLOOK

Three-dimensional QED is an interesting field theory due to its similarities to four-dimensional QCD-like theories and its applications in high temperature superconductivity. In this paper we presented the first results from lattice simulations with massless fermions of noncompact QED_3 coupled to a weak Z_2 chirally invariant four-fermi interaction. Below we summarize and discuss our main findings.

The values of the critical exponents β_m and δ extracted from simulations with $N_f \geq 4$ are close to the values of the respective $3d$ Gross-Neveu exponents. This implies that even for very weak four-fermi couplings (almost 20 times smaller than the pure Gross-Neveu critical coupling) the strong coupling chiral transition/crossover for $N_f \geq 4$ is dominated by the Gross-Neveu ultraviolet-stable renormalization group fixed point. The gauge interaction is an irrelevant operator near the transition, but the system can be driven towards (pseudo-)criticality by varying the gauge coupling. It is noted that certain values of the critical exponents (especially δ) extracted from simulations with the strongest four-fermi coupling, $\beta_s = 2$ are slightly larger than those of the pure Gross-Neveu exponents, which hints at preliminary evidence for nonzero fermion mass generated by the gauge field dynamics. Future large-scale simulations will further clarify this issue. In the weak four-fermi coupling limit the $N_f = 4$ critical gauge coupling β_c is significantly smaller than its respective pure $N_f = 4$ QED_3 value, possibly because the four-fermi term forbids lattice discretization counter-terms that may exist in the pure QED_3 effective action with $m \neq 0$. Furthermore, for a given N_f value, in the weak four-fermi coupling limit the scaling region is suppressed by a factor $\sim 1/\sqrt{\beta_s}$, whereas for fixed β_s and variable N_f the scaling region is suppressed by a factor $\sim\sqrt{\beta_{\text{cross}}(N_f)/N_f}$. Also, the effects of the four-fermi coupling on the monopole density are smaller than on the chiral condensate, as ρ_m depends more strongly on the short-distance fluctuations of the gauge field, whereas the fermion condensate is significantly enhanced near the transition by the four-fermi coupling. For $N_f \geq 4$ we have also seen evidence that at strong couplings the chiral condensate is correlated to the monopole density in an N_f-independent manner.

We also reached the conclusion that the monopoles are shielded at weak couplings for $N_f \geq 1$ because: (i) the monopole polarizability measured by χ_m showed no signs of a divergent behavior, and (ii) the exponential decrease of the isolated monopoles' density with β is faster than the decrease of the total density of positive magnetic charges. A comparison of our results with those from simulations of compact QED_3 coupled to a four-fermi term [29] which favor survival of the monopole plasma at weak couplings for $N_f = 4$ implies that the monopole dynamics in the two models are different.

The various results from this first exploratory study are promising. This is due to the presence of the four-fermi coupling in the model's action, which increased substantially the efficiency of the simulation algorithm. In the near future we plan to extend this work in the following directions: (i) Large scale simulations of the noncompact version with $N_f \leq 4$ to compare the scaling properties at the transition/crossover with those of pure Gross-Neveu model. Possible deviations may provide evidence for the existence of fermion mass generated by the gauge field dynamics. (ii) Landau gauge-fixed simulations to measure the fermion dynamical mass, which according to SDE approaches it is expected to be an order of magnitude smaller than the natural cutoff scale e^2 in the continuum limit [15], and hence significantly larger than the chiral condensate. (iii) Simulations of compact QED_3 with different values of N_f and comparison with the existing analytical results.

ACKNOWLEDGMENTS

The authors are grateful to Simon Hands and Pavlos Vranas for valuable insight and discussions. J. B. K. thanks the National Science Foundation for providing computer time at several NSF supported computer centers under

Grant No. MCA99S015. The authors also wish to thank Diamond Light Source for kindly allowing them to use extensive computing resources, specifically Tina Friedrich, Frederik Ferner, James Rowland and Alun Ashton for help in configuring and maintaining these resources. W. A. would like to thank Gwyndaf Evans for his support and useful advice.

[1] B. Holdom, Phys. Lett. B **150**, 301 (1985); K. Yamawaki, M. Bando, and K. Matumoto, Phys. Rev. Lett. **56**, 1335 (1986); T. Appelquist, D. Karabali, and L. C. R. Wijewardhana, Phys. Rev. Lett. **57**, 957 (1986).
[2] R. Pisarski, Phys. Rev. D **29**, 2423 (1984).
[3] T. Appelquist, D. Nash, and L. C. R. Wijewardhana, Phys. Rev. Lett. **60**, 2575 (1988); P. Maris, Phys. Rev. D **54**, 4049 (1996); C. S. Fischer, R. Alkofer, T. Dahm, and P. Maris, Phys. Rev. D **70**, 073007 (2004); D. Nash, Phys. Rev. Lett. **62**, 3024 (1989); K.-I. Kondo, T. Ebihara, T. Iizuka, and E. Tanaka, Nucl. Phys. **B434**, 85 (1995); I. Aitchison, N. Mavromatos, and D. McNeill, Phys. Lett. B **402**, 154 (1997).
[4] T. Goecke, C. S. Fischer, and R. Williams, Phys. Rev. B **79**, 064513 (2009).
[5] M. Pennington and D. Walsh, Phys. Lett. B **253**, 246 (1991).
[6] K. Kaveh and I. F. Herbut, Phys. Rev. B **71**, 184519 (2005).
[7] A. Bashir, A. Raya, S. Sanchez-Madrigal, and C. D. Roberts, Few-Body Syst. **46**, 229 (2009).
[8] T. Appelquist, A. Cohen, and M. Schmaltz, Phys. Rev. D **60**, 045003 (1999).
[9] N. Mavromatos and J. Papavassiliou, arXiv:cond-mat/0311421.
[10] T. Appelquist, J. Terning, and L. C. R. Wijewardhana, Phys. Rev. Lett. **75**, 2081 (1995); V. P. Gusynin, V. A. Miransky, and A. V. Shpagin, Phys. Rev. D **58**, 085023 (1998).
[11] S. Hands and J. B. Kogut, Nucl. Phys. **B335**, 455 (1990).
[12] S. J. Hands, J. B. Kogut, L. Scorzato, and C. G. Strouthos, Phys. Rev. B **70**, 104501 (2004).
[13] C. Strouthos and J. B. Kogut, J. Phys. Conf. Ser. **150**, 052247 (2009).
[14] S. J. Hands, J. B. Kogut, and C. G. Strouthos, Nucl. Phys. **B645**, 321 (2002).
[15] A. Bashir and A. Raya, Few-Body Syst. **41**, 185 (2007).
[16] V. P. Gusynin and M. Reenders, Phys. Rev. D **68**, 025017 (2003).
[17] S. Hands, Phys. Rev. D **51**, 5816 (1995).
[18] S. Christofi, S. Hands, and C. Strouthos, Phys. Rev. D **75**, 101701 (2007).
[19] E. Dagotto, A. Kocic, and J. B. Kogut, Nucl. Phys. **B334**, 279 (1990).
[20] T. Appelquist, M. J. Bowick, E. Cohler, and L. C. R. Wijewardhana, Phys. Rev. Lett. **55**, 1715 (1985).
[21] N. Dorey and N. E. Mavromatos, Nucl. Phys. **B386**, 614 (1992).
[22] V. Gusynin, A. Hams, and M. Reenders, Phys. Rev. D **63**, 045025 (2001).
[23] M. Franz and Z. Tesanovic, Phys. Rev. Lett. **87**, 257003 (2001); Z. Tesanovic, O. Vafek, and M. Franz, Phys. Rev. B **65**, 180511 (2002); I. F. Herbut, Phys. Rev. B **66**, 094504 (2002); A. Concha, V. Stanev, and Z. Tesanovic, Phys. Rev. B **79**, 214525 (2009).
[24] S. Hands and I. O. Thomas, Phys. Rev. B **72**, 054526 (2005); **75**, 134516 (2007).
[25] S. Kim, J. B. Kogut, and M. P. Lombardo, Phys. Lett. B **502**, 345 (2001); Phys. Rev. D **65**, 054015 (2002).
[26] J. B. Kogut and C. G. Strouthos, Phys. Rev. D **67**, 034504 (2003); **71**, 094012 (2005).
[27] B. Rosenstein, B. Warr, and H. Park, Phys. Rev. Lett. **62**, 1433 (1989); S. Hands, A. Kocic, and J. Kogut, Ann. Phys. (N.Y.) **224**, 29 (1993).
[28] J. B. Kogut, C. G. Strouthos, and I. N. Tziligakis, Nucl. Phys. B, Proc. Suppl. **140**, 701 (2005).
[29] S. Hands, J. B. Kogut, and B. Lucini, arXiv:hep-lat/0601001.
[30] S. Hands and R. Wensley, Phys. Rev. Lett. **63**, 2169 (1989).
[31] J. L. Cardy, Nucl. Phys. **B170**, 369 (1980).
[32] T. A. DeGrand and D. Toussaint, Phys. Rev. D **22**, 2478 (1980).
[33] M. Salmhofer and E. Seiler, Commun. Math. Phys. **139**, 395 (1991); **146**, 637(E) (1992).
[34] S. Christofi and C. Strouthos, J. High Energy Phys. 05 (2007) 088.
[35] U. Mahanta, Phys. Rev. D **44**, 3356 (1991).
[36] L. Karkkainen, R. Lacaze, P. Lacock, and B. Petersson, Nucl. Phys. **B415**, 781 (1994); **B438**, 650(E) (1995); E. Focht, J. Jersak, and J. Paul, Phys. Rev. D **53**, 4616 (1996).
[37] I. F. Herbut, Phys. Rev. Lett. **97**, 146401 (2006); V. Juricic, I. Herbut, and G. Semenoff, Phys. Rev. B **80**, 081405 (2009).
[38] G. Calucci and R. Jengo, Nucl. Phys. **B223**, 501 (1983).
[39] H. R. Fiebig and R. M. Woloshyn, Phys. Rev. D **42**, 3520 (1990).
[40] R. Fiore, P. Giudice, D. Giuliano, D. Marmottini, A. Papa, and P. Sodano, Phys. Rev. D **72**, 094508 (2005).
[41] J. Martson, Phys. Rev. Lett. **64**, 1166 (1990).
[42] H. Kleinert, F. S. Nogueira, and A. Sudbø, Phys. Rev. Lett. **88**, 232001 (2002); F. S. Nogueira and H. Kleinert, Phys. Rev. Lett. **95**, 176406 (2005).
[43] F. S. Nogueira and H. Kleinert, Phys. Rev. B **77**, 045107 (2008).
[44] I. F. Herbut and B. H. Seradjeh, Phys. Rev. Lett. **91**, 171601 (2003); M. J. Case, B. H. Seradjeh, and I. F. Herbut, Nucl. Phys. **B676**, 572 (2004).